Case Studies in Construction Materials 14 (2021) e00541

Contents lists available at ScienceDirect

Case Studies in Construction Materials

journal homepage: www.elsevier.com/locate/cscm

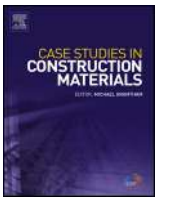

Case study

Improving the compressive behavior of RC walls reinforced with ferrocement composites under centric and eccentric loading

Abeer M. Erfan, Ragab M. Abd Elnaby, Ammar Elhawary, Taha A. El-Sayed*

Department of Structural Engineering, Shoubra Faculty of Engineering, Benha Univeristy, 108 Shoubra Street, Shoubra, Cairo, Egypt

ARTICLE INFO

Article history:
Received 21 December 2020
Received in revised form 23 March 2021
Accepted 25 March 2021

Keywords:
Ferrocement composites
Compression loading
Concentric load
Eccentric load
RC walls
Welded wire mesh
Ductility index
Energy absorption
Ansys 2019-R1

ABSTRACT

This study discusses the behavior of reinforced concrete (RC) walls reinforced with different types of ferrocement composites under concentric and eccentric loading. The study incorporated experimental examination and nonlinear finite element analysis of ten RC walls with dimensions of 1000 mm in height, 1500 mm in width, and 150 mm in depth with RC footing with dimensions 1900 mm X 500 mm X 200 mm. The specimens were divided into two groups, one examined under concentric load and the other examined under eccentric load with eccentricity of 50 mm. Also, the structural behavior of the tested walls was validated with numerical development of a finite element model utilizing Ansys 2019-R1 software. Expanded or glass fiber wire mesh ferrocement tested specimens under concentric and eccentric line compression loading exhibited enhanced ultimate loads compared to control specimens. Expanded steel wire mesh reinforcement increased the ductility ratio compared to glass fiber mesh reinforcement. Glass fiber wire mesh produced a higher first cracking load, serviceability load, load carrying capacity, and energy absorption compared to expanded wire mesh. Good agreement between numerical and experimental results in first cracking load, load-carrying capacity, crack pattern, and deflection was found. The agreement between the experimental load carrying capacity and non linear finite element (NLFE) ones is about 86 % with coefficient of variance equals 0.003 and standard deviation of 0.06. The finite element analysis gave suitable estimation for the structural performance of nonlinear ferrocement RC walls.

1. Introduction

Ferrocement is classified to construct thin reinforced concrete (RC) walls generally created with cement mortar reinforced with separate layers of tiny diameter wire mesh. It has been widely applied to build various element such as walls, tanks, roofs, and bridge decks [1–9]. For reinforced concrete structures, the walls are the most important and critical element and can determine the behavior and failure mode of the structure. Recently, breakdown of RC structures has occurred because of large working loads, seismic loads, and durability challenges. The economic losses due to such failures amount to billions of dollars.

Mansur and Paramasivan [10] conducted an experimental study on box-section ferrocement columns under centric and eccentric compression loading. The main task of ferrocement in most concrete elements is to modify the cracking

* Corresponding author. Tel:+20 1008444985, Website: http://www.bu.edu.eg/staff/tahaibrahim3.
E-mail address: taha.ibrahim@feng.bu.edu.eg (T.A. El-Sayed).

https://doi.org/10.1016/j.cscm.2021.e00541

Table 1
Mechanical properties of meshes.

Mesh type	Tensile strength (MPa)	Young's modulus (MPa)	Opening dimensions (mm)	Diameter (mm)
Expanded wire.	250	12,000	16.5 × 31.0	1.25
Glass fiber wire	230	8000	1.66 × 0.66	0.66

mechanism. By modifying the crack mechanism, it has been shown that with microcracking [11–16] the cracks have a smaller width; this reduces the permeability of the concrete and improves the tensile strength. A great advantage of using ferrocement composite reinforced concrete to reduce permeability and increase fatigue resistance is that the addition of fibers improves the toughness or load capacity. In addition, numerous studies have shown that the impact strength of concrete can also be significantly improved by adding fibers to the concrete mix.

On the other hand, many studies have been done on RC columns reinforced by ferrocement. They studied circular and square short columns reinforced with ferrocement composites and concluded that ferrocement reinforcement enhanced the columns' load carrying capacity and ductility for centric and eccentric compression loading [17–20].

Because concrete walls are important as a main element in concrete structures, there is a need to develop and investigate new materials used in wall casting to enhance the performance of concrete structures until collapse. Using innovative ferrocement composites will partly satisfy the need to enhance wall behavior under centric and eccentric loads and increase strength, ductility, and energy absorption.

Commonly, traditional procedures of improving the structures load capacity and ductility are concrete steel jacketing [21–23]. Several researchers had been studied the glass fiber reinforced polymer (GFRP) composites [24]. Lately, Yan & Pimanmas et al., studied the axial compressive of NFRP concrete [25,26] and told that natural fiber reinforced polymer (NFRP) was very useful to the performance of confined concrete.

For PVC walls subjected to both axial and eccentric loading, the polymer enhanced the tensile strength capacity for all samples [27,28]. This system may be used for retaining walls, shear walls and water structures walls. These walls are subjected for both axial and eccentric loading.

2. Experimental program

This investigation was carried out to study the effect of using ferrocement composites to reinforce concrete walls under centric and eccentric compression loading. This experiment was done at the Housing and Building National Research Center (HBNRC), Dokki, Egypt. The aim of this study was to estimate the ultimate load, deflection, strains in concrete, cracks and their propagation, energy absorption, and ductility ratio.

2.1. Experimental study

2.1.1. Materials

- Cement: OPC type I (CEM 42.5 N), produced by the Suez cement factory, Egypt.

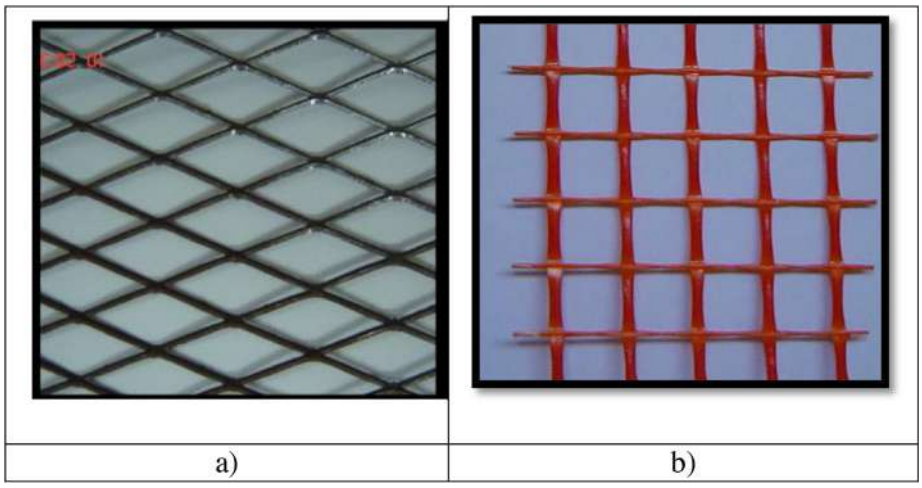

Fig. 1. Configuration of ferrocement composites: (a) expanded wire mesh.
(b) glass fiber wire mesh.

Table 2
Concrete mixes and material weights.

Material	f_{cu} =40 MPa
Cement	400 kg/m^3
Coarse aggregate	1407 kg/m^3
Fine aggregate	594 kg/m^3
Water	168 kg/m^3
Super plasticizer	4.0 kg/m^3

Fig. 2. Slump test.

- Fine aggregate: Natural siliceous sand with a specific gravity 2.6 t/m^3 and a modulus of fineness 2.7.
- Coarse aggregate: 10 mm maximum aggregate size, crushed stone aggregate with a specific gravity 2.89 t/m^3,
- Water: fresh water free used for mixing and curing.
- Super plasticizer: A high range water reducer HRWR produced by CMB GROUP under the commercial name of Addicrete BVF with amount of 1.0 % of the cement weight.
- Reinforcing steel: High grade Ezz Al-Dekhila Steel, Alexandria, Egypt, 36/52 (deformed bars) of diameter 10 and 12 mm.
- Ferrocement composite wire mesh: Table 1 showed the properties of composite wire mesh used instead of steel reinforcement. Fig. 1 showed two sorts of meshes (expanded and glass fiber wire mesh) were employed as ferrocement reinforcement. Expanded wire mesh with a diamond size of 16.5 × 31.0 mm and weight of 1660 g/m^2 was used. Glass fiber mesh with dimensions of 1.66 × 0.66 mm was employed. The configuration of ferrocement composites as in Table 1.

2.1.2. Concrete mix

One concrete mix was used in the experimental program with compressive strength of 40 MPa. The weights of materials used are presented in Table 2. Six concrete cubes were poured during the pouring of concrete slabs.

2.1.3. Workability

Super plasticizer added to the mix to improve the workability for a suitable slump. Fig. 2 showed the slump for concrete used.

2.1.4. Compressive strength test

Compressive strength test was performed on three cube specimens 150 × 150 × 150 mm^3. Specimens were examined after 28 days. A 2000 kN capacity testing machine was utilized for the testing as in Fig. 3. The compressive strength results as in Table 3.

2.1.5. Description of tested walls

The experimental program consisted of two groups of concrete walls with the same dimensions. Each group was divided into five concrete walls; the first was the control specimen, which was reinforced using steel bars in the longitudinal and

Fig. 3. Crushing machine of cubes specimens.

Table 3
Compressive strength test results.

Cubes	Compressive Strength (MPa) 28 days
C1	43.9
C2	45.2
C3	42.7
Avg.	**43.9**

horizontal direction, and the other four specimens had expanded and glass fiber wire mesh instead of horizontal steel reinforcement. This group was examined under concentric compression loading, and the second group was examined under eccentric loads, as shown in Table 4 and Fig. 4. Also, the wall dimensions & designed reinforcement details as in Fig. 5.

2.2. Test setup

The concrete walls were tested under line load. The test was done at the Housing and Building National Research Center (HBNRC), Dokki, Egypt, under a testing machine with 5000 kN maximum capacity, as indicated in Fig. 6. The load was incrementally applied to the specimens. Strain gauges with accuracy of 0.005 mm were placed as shown in Fig. 7 and LVDTs were used to record the deflection of slabs at mid-span and at 200 mm from supports. The load was increased until failure, and the load strain and deflection were recorded.

3. Experimental results and discussion

The performance of concrete walls reinforced with different composite wire mesh materials was analyzed. The compressive strength and combined behavior due to concentric and eccentric load were examined, as well as load-carrying

Table 4
Specimens details.

Specimen group	Specimen symbol	Type of load test	Horizontal RFT. type	Reinforcement	
				Ver. RFT.	Hzl. RFT.
Group I	W1	Concentric	Steel RFT	6φ12/m	6φ10/m
	W1−1	Concentric	Expanded wire mesh	6φ12/m	One layer
	W1−2	Concentric	Expanded wire mesh	6φ12/m	Two layers
	W1−3	Concentric	Glass fiber wire mesh	6φ12/m	Two layers
	W1−4	Concentric	Glass fiber wire mesh	6φ12/m	Four layers
Group II	W2	Eccentric	Steel RFT	6φ12/m	6φ10/m
	W2−1	Eccentric	Expanded wire mesh	6φ12/m	One layer
	W2−2	Eccentric	Expanded wire mesh	6φ12/m	Two layers
	W2−3	Eccentric	Glass fiber wire mesh	6φ12/m	Two layers
	W2−4	Eccentric	Glass fiber wire mesh	6φ12/m	Four layers

Fig. 4. Specimen configurations: (a) control wall; (b) wall with expanded wire mesh; (c) wall with glass fiber mesh.

capacity, crack pattern, and concrete stress–strain curves, and finally the specimen's volume friction and energy absorption were analyzed.

3.1. Ultimate experimental failure load

The experiment was divided into two groups. The first group, tested under concentric loading, consisted of five concrete walls; the control failed at an ultimate load of 1950.0 kN but the failure load of walls W1−1 and W1−2, which used expanded wire mesh of one and two layers, was 2033.0 kN and 2541.0 kN, respectively. For specimens W1−3 and W1−4, which used glass fiber mesh instead of horizontal reinforcement, the failure load was 1944.0 kN and 2040.0 kN, respectively. The enhancement in failure load was 4.25 %, 30.3 %, 0.0 %, and 4.62 % for W1−1, W1−2, W1−3, and W1−4, respectively. This showed the effect of using expanded wire mesh to enhance the failure load capacity, which was agreed with Fahmy et al. [16–18]

The second group of concrete walls was tested under eccentric load of 50 mm. Specimen W2 was the control, which failed at a load of 936.0 K N. For the other specimens reinforced with expanded and glass fiber wire mesh, the failure load was 1392.0 kN, 1928.0 kN, 1775.0 kN, and 1906.0 kN for W2−1, W2−2, W2−3, and W2−4, respectively. The enhancement ratio of failure load in this group is relatively higher than that of the first group, at 48.7 %, 105.9 %, 89.6 %, and 103.6 %, respectively, which was agreed with Fahmy et al. [16–18]. This indicates the effect of using this type of ferrocement composite in eccentric loads, as shown in Table 5 and Fig. 8.

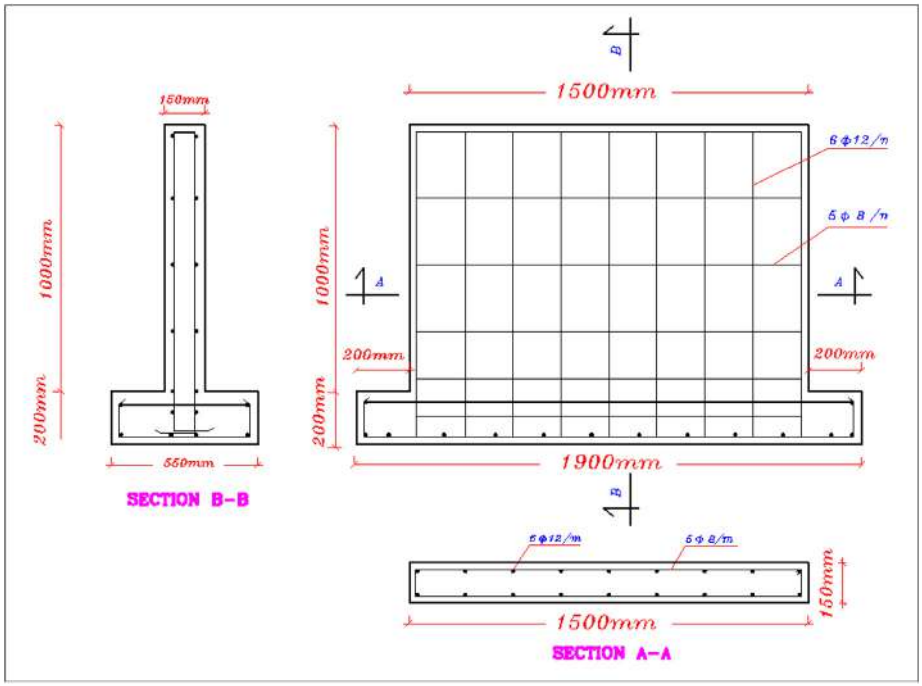

Fig. 5. Wall dimensions & designed reinforcement details.

Fig. 6. Test setup.

3.2. Cracking

Typically, the first crack in all tested walls in the vertical stage of loading developed in the loaded surface. For the first group tested under concentric loads, cracks in the control specimen started at 850 kN at the head at the point of load concentration, then it was still and propagated suddenly at the maximum load of 1950 kN. After this the load decreased and the cracks increased with the loading rate, showing failure of the wall. Specimens W1–1, W1–2, W1–3, and W1–4 recorded

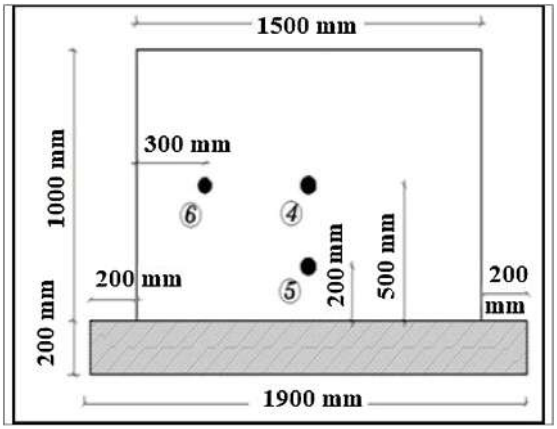

Fig. 7. Strain gauge positions.

Table 5
Experimental results of tested walls.

Specimen group	Specimen symbol	Type of load test	Ultimate load (kN)		Volume friction (%)	Enhancement ratio (%) ($\frac{Pu-Pu\ control}{Pu\ control}$ x 100)	
			First crack	Failure load		First crack	Failure load
Group I	W1	Concentric	850.0	1950.0	1.95	–	–
	W1–1	Concentric	1500.0	2033.0	1.02	76.4	4.25
	W1–2	Concentric	1800.0	2541.0	1.05	111.7	30.3
	W1–3	Concentric	1020.0	1944.0	1.01	20.0	0.0
	W1–4	Concentric	1025.0	2040.0	1.01	20.1	4.62
Group II	W2	Eccentric	610.0	936.0	1.95	–	–
	W2–1	Eccentric	620.0	1392.0	1.02	1.63	48.7
	W2–2	Eccentric	740.0	1928.0	1.05	21.30	105.9
	W2–3	Eccentric	648.0	1775.0	1.01	6.23	89.60
	W2–4	Eccentric	700.0	1906.0	1.01	1.47	103.6

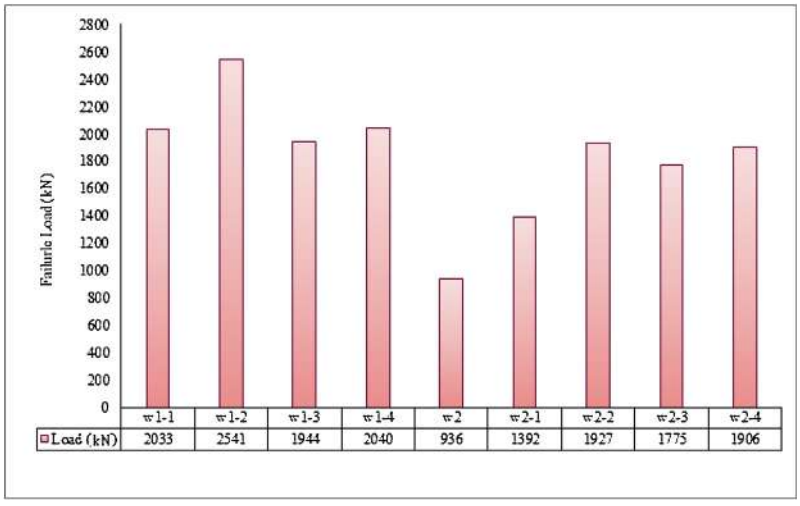

Fig. 8. Comparison of experimental failure loads.

an enhancement in crack load of 76.4 %, 111.7 %, 20.0 %, and 20.1 %, respectively, compared to the control wall (W1), as indicated in Table 5 and Fig. 9.

For the second group in the eccentric loading test, the enhancement in cracking load was less than in the first group related to the load eccentricity. The first crack in specimen W2 appeared at a load of 610.0 kN at the head at the point of load concentration, then it was still and propagated suddenly at the maximum load of 936.0 kN. After this the load decreased and

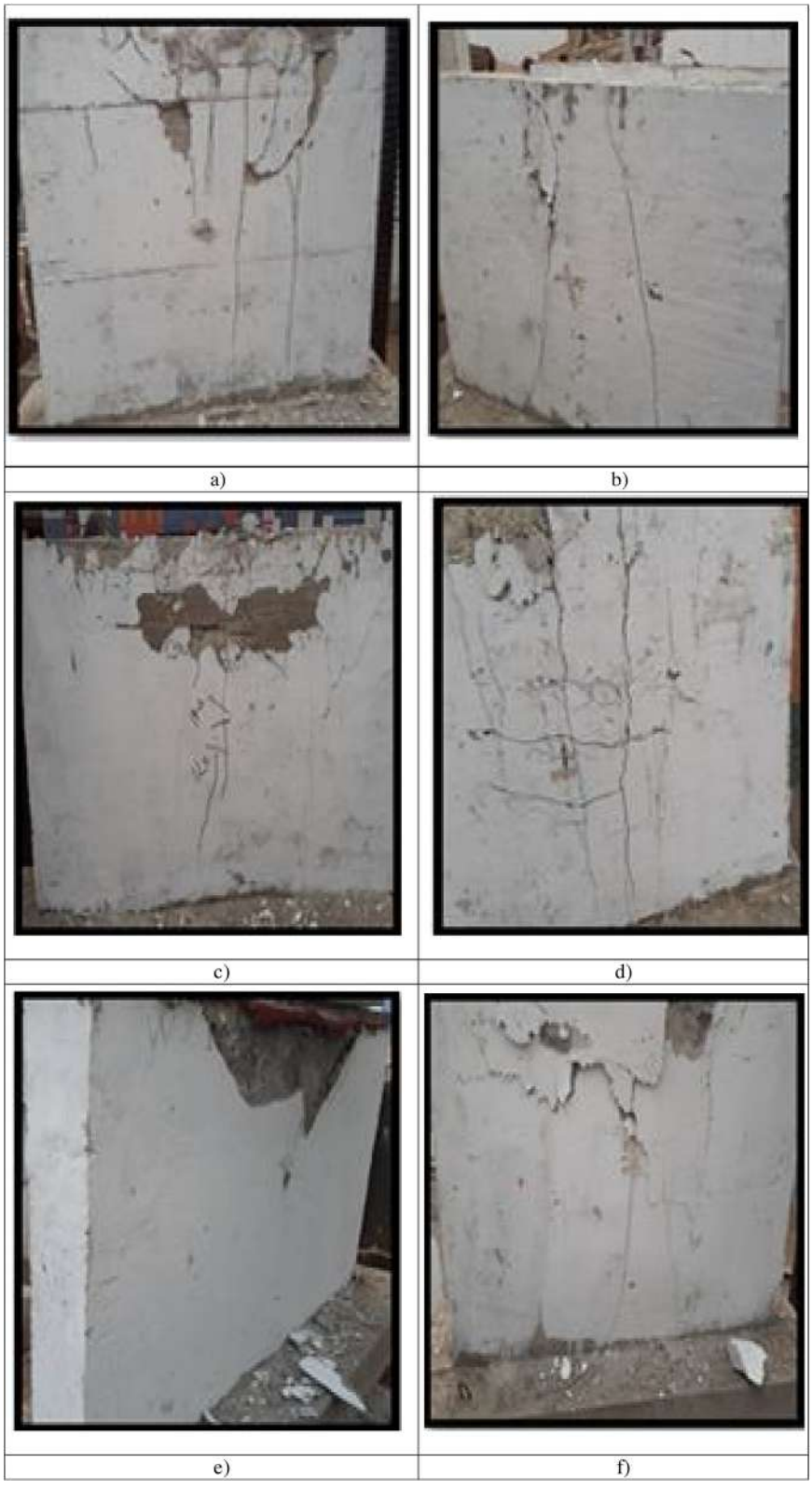

Fig. 9. Crack patterns of tested walls: (a) W1; (b) W1-2; (c) W1-4; (d) W2; (e) W2-2; (f) W2-4.

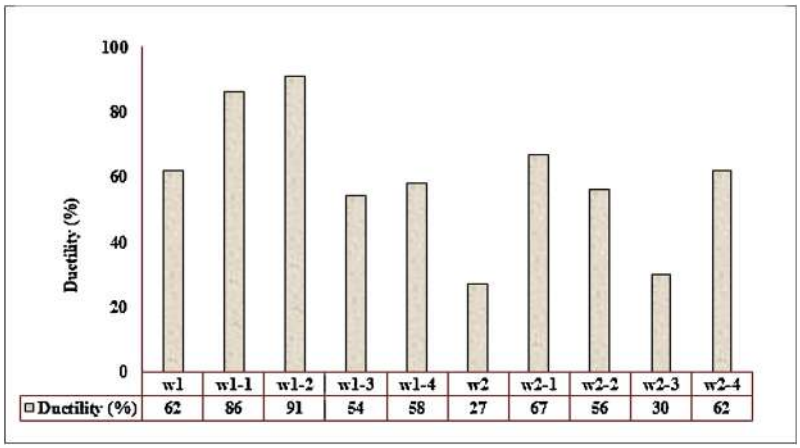

Fig. 10. Ductility of tested walls.

the cracks increased with the loading rate, showing failure of the wall. For specimens W2−1, W2−2, W2−3, and W2−4, the enhancement of cracks was 1.63 %, 21.6 %, 6.26 %, and 1.47 %, respectively, compared to the control. This showed the effect of using expanded wire mesh to reinforce the RC wall, as horizontal reinforcement showed a high effect compared to glass fiber composite which was agreed with Fahmy and Hazem [18,20]

3.3. Volume fraction of steel reinforcement

Experimental results reveal that increased volume fraction of steel reinforcement contributed to the slightly higher ultimate load. This is clear when comparing wall W1 and the other walls, showing different degrees of increase in the ultimate failure load, however the increase in steel volume fraction resulted in much stiffer specimens, as shown in Table 5.

3.4. Ductility ratio

Ductility was calculated by the ratio between the deflection of the tested wall at 0.8 of ultimate load to the mid-span displacement at the ultimate failure load. Walls reinforced with expanded metal mesh and glass fiber wire mesh had a higher ductility ratio than control walls W1 and W2. Specimen W1−2 had a higher ductility ratio with respect to the control in the first group, which was agreed with Fahmy, E.H. et al. [16–18]. Table 5 and Fig. 10 showed the ductility ratio for all tested walls.

3.5. Energy absorption

Energy absorption was obtained by calculating the area under the load–deflection curve for each wall. Walls reinforced with expanded steel mesh achieved higher energy absorption than control walls. Table 5 and Fig. 11 highlighted energy

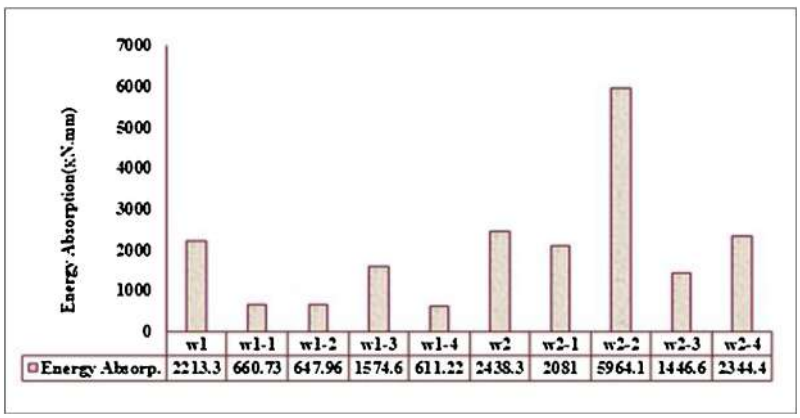

Fig. 11. Energy absorption of tested walls.

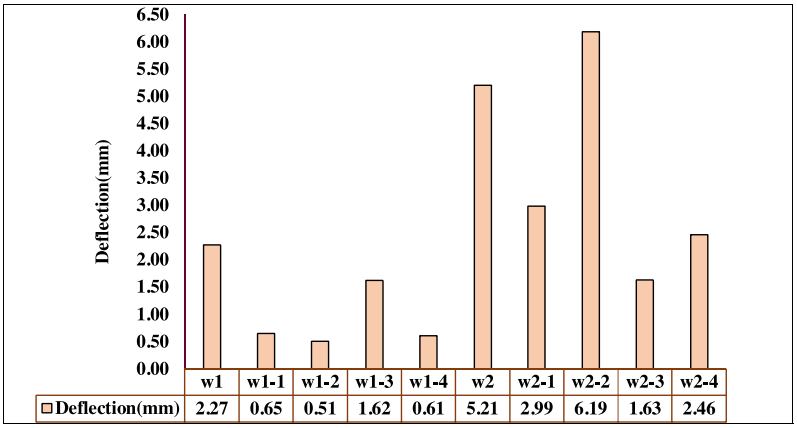

Fig. 12. Comparison of obtained deflection of tested walls.

absorption for all tested specimens with greater properties of energy absorption and ductility, which are useful for dynamic purposes.

3.6. Lateral deflection of tested walls

The behavior of the tested specimens in terms of the load–deflection relationship is discussed in the following sections. The load–deflection curve of control specimen W1, tested under concentric loads, was recorded as 2.27 mm. The use of ferrocement layers, especially expanded and glass fiber types, showed good enhancement in deflection, as shown in Figs. 12 & 13 . The enhancement in deflection for this group varied between 77.5 % and 28.6 %, as indicated in Table 6.

For concrete walls tested under eccentric loads, high deflection was recorded with respect to the other group. Specimen W2 recorded a deflection of 5.21 mm, whereas the values were 2.99, 6.19, 1.63, and 2.46 mm for W2−1, W2−2, W2−3, and W2−4, respectively. Specimen W2−2 appeared to have a high deflection value due to its high failure load and eccentricity. The enhanced deflection for this group varied between 27.0 % and 62.0 %, as given in Table 6 and Figs. 12 and 13.

The use of ferrocement composites indicated an enhancement in the deflection of tested walls, especially under concentric loads, which was agreed with Mansur and Paramasivam [10]

4. Nonlinear finite element analysis

Nonlinear finite element analysis (NLFEA) was carried out to investigate the behavior of reinforced concrete walls using expanded and glass fiber wire mesh employing Ansys 2019-R1 software [29]. The discussed behavior includes the crack pattern, ultimate load, and load–deflection response of the test specimens.

4.1. Reinforced concrete wall modelling

NLFEA was conducted for the reinforced concrete walls with innovative composites. Ansys 2019- R1 has several three-dimensional elements in its library. In this study, SOLID 65 for concrete was used with mesh size 50 mm. The steel bars were formed by applying the LINK 180 3-D element. Fig. 14 showed the geometry and for Solid 65 & LINK 180 elements. Ferrocement materials were modeled by using the volumetric ratio in the concrete element. The concrete compressive strength was 40 MPa.

4.2. Verification of model

In this research, the FEA examined cracking, yielding of the steel and failure strength of the RC walls. Newton-Raphson method was used for the non-linear response of analysis. Load was increased incrementally till un-convergence which means that failure occurred.

4.3. Material properties

For **concrete**:
Elastic modulus of elasticity: based on ECP 203/2018 [30].
($E_c = 4400\sqrt{f_{cu}} = 24{,}100$ N/mm2)
& Poisson's ratio ($\nu = 0.3$)

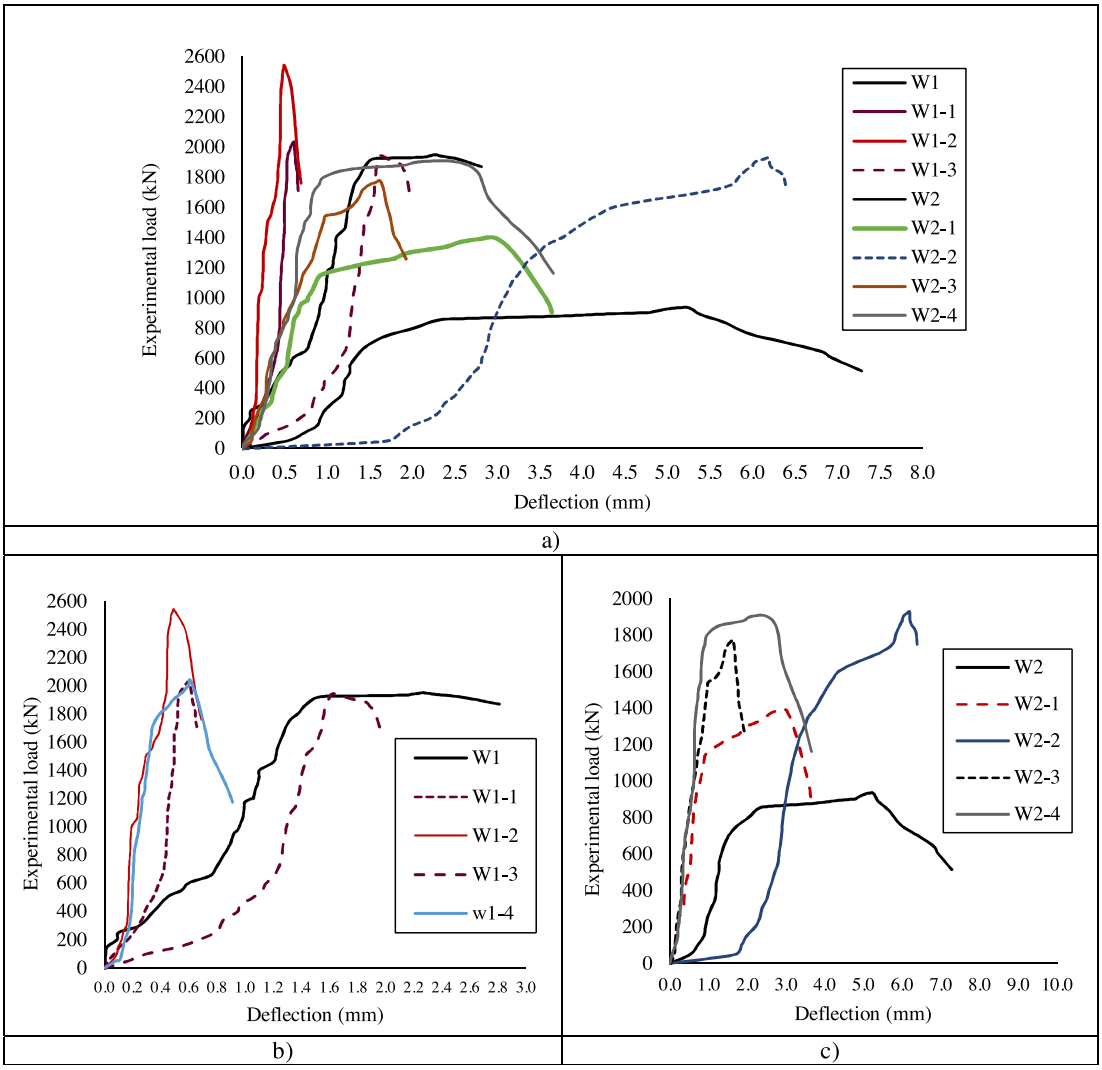

Fig. 13. Load–deflection curves for tested walls: (a) all specimens; (b) specimens under concentric load; (c) specimens under eccentric load.

For **reinforcing steel** bars: based on ECP 203/2018 [30].

1 Elastic Modulus of elasticity (E_s = 200 kN/mm2)
2 Yield stress (f_y = 360 N/mm2)
3 Poisson's ratio (ν = 0.2)
4 Area of steel for φ10 (As = 78.5 mm2)
5 Area of steel for φ12 (As = 112 mm2)

For **wire mesh** reinforcement:

-1
Expanded wire mesh.

Yield stress (f_y = 250 N/mm2): as per manufacturer.

Volumetric ratio

- The diameter of mesh wire ($\mathbf{d_w}$) = 1.25 mm
- Area / mm^2 = **1.227** mm^2

Table 6
Comparison of obtained results.

Specimen group	Specimensymbol	Ultimate deflection		Ductility ratio (%)	Energy absorption (kN.mm)	Enhancement (%) $(\frac{\Delta u - \Delta u\ control}{\Delta u\ control}\ x\ 100)$
		0.8 Δu_{exp}	Δu_{exp}			
Group I	W1	1.23	2.27	62.0	2213.25	–
	W1−1	0.4	0.65	86.0	660.725	71
	W1−2	0.44	0.51	91.0	647.955	77.5
	W1−3	1.48	1.62	54.0	1574.64	28.6
	W1−4	0.33	0.61	58.0	611.22	73.1
Group II	W2	3.02	5.21	27.0	2438.28	–
	W2−1	0.8	2.99	67.0	2081.04	42.6
	W2−2	4.12	6.19	56.0	5964.065	18.8
	W2−3	0.91	1.63	30.0	1446.625	68.7
	W2−4	0.73	2.46	62.0	2344.38	52.8

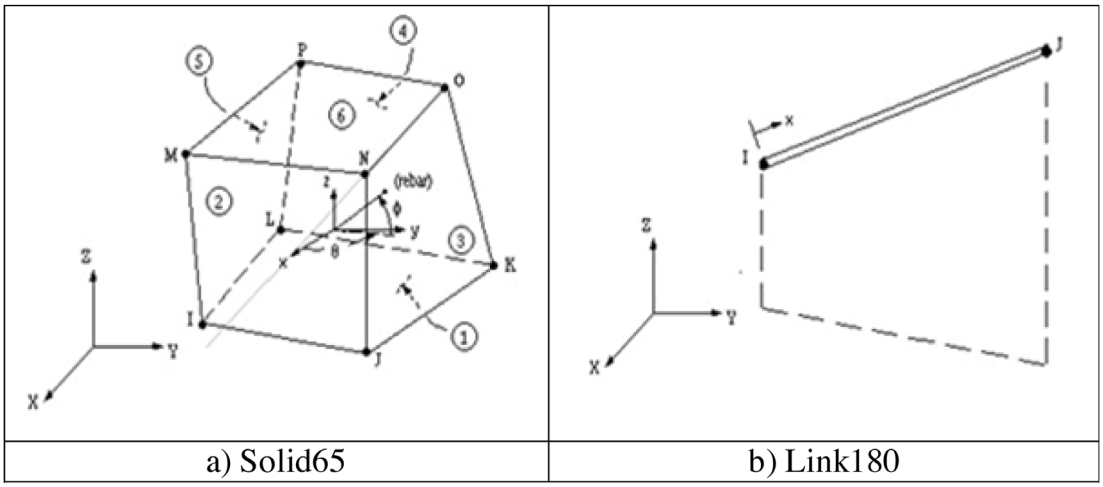

Fig. 14. Geometry & node locations for element types.

- Total area (**one layer)** = 13.938 mm^2

  Volumetric ratio of one layer = 0.0093

- Volumetric ratio of one layer = 0.0093
- Volumetric ratio of two layers = 0.0186

-1 **Fiber glass wire mesh**

Yield stress (f_y = 230 N/mm2): as per manufacturer.

Volumetric ratio

- The diameter of wire mesh ($\mathbf{d_w}$) = 0.66 mm
- Area / mm^2 = **0.342** mm^2
- Total area (**one layer)** 4.6158 mm^2

  Volumetric ratio of one layer = 0.0031

- Volumetric ratio of two layers = 0.0062
- Volumetric ratio of three layers = 0.0124

4.4. Material properties

NLFEA was carried out to study the behavior of RC walls reinforced with different types of ferrocement composites under concentric and eccentric loading using software ANSYS 2019-R1. RC walls NLFE modeling as in Fig. 15.

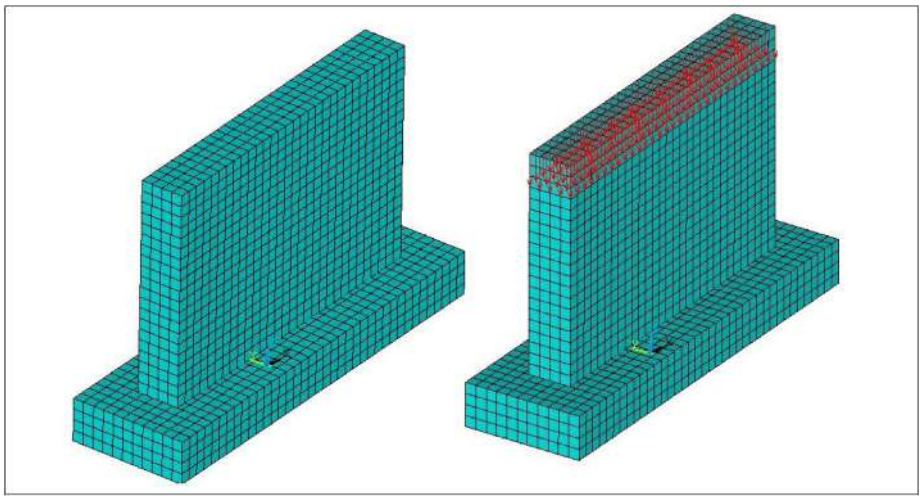

Fig. 15. Nonlinear finite element analysis (NLFEA) 3D model of RC walls with mesh size 50 mm.

Table 7
NLFEA results of failure load and deflection.

Specimen group	Specimensymbol	NLFEA of loads (kN)		NLFEA of deflection (mm)	Enhancement ratio (%) ($\frac{Pu-Pu\ control}{Pu\ control}$ x 100)	
		First crack	Failure load		Deflection	Failure load
Group I	W1	320.0	1755	2.04	–	–
	W1–1	320.0	1931.35	0.62	30.4	10.0
	W1–2	320.0	2159.85	0.43	21.1	23.0
	W1–3	320.0	1691.28	1.41	69.1	3.63
	W1–4	320.0	1856.4	0.55	27.0	5.78
Group II	W2	285.0	795.6	4.43	–	–
	W2–1	285.0	1044	2.24	49.3	31.2
	W2–2	285.0	1657.22	5.32	20.2	108.2
	W2–3	285.0	1402.25	1.30	70.9	76.3
	W2–4	285.0	1620.1	2.10	52.8	103.6

4.5. NLFEA ultimate failure load

Ultimate loads obtained from NLFEA were recorded for the first group of concrete walls under eccentric load and compressive strength of concrete at 40 MPa. Specimen W1 was the control specimen. Failure load $P_{U\ NLFEA}$ was 1755.0 kN.

For the first group of concrete walls, which were reinforced with one and two layers of expanded wire mesh for W1–1 and W1–2, the failure load was 1931.0 kN and 2159.8 kN, respectively. For walls reinforced using glass fiber mesh, the failure load was 1691.0 kN and 1856.4 kN for W1–3 and W1–4, respectively. The enhancement ratio in this group varied between 3.23 % and 23.0 %, as shown in Table 7.

For the second group of concrete walls, which were tested under eccentric load, the failure load was 795.6 kN, 1044 kN, 1657.2 kN, 1402.2 kN, and 1620.1 kN for W2, W2–1, W2–2, W2–3, and W2–4, respectively. The enhancement ratio of walls tested under eccentric load was 31.2 %, 108.2 %, 76.3 %, and 103.6 % for W2–1, W2–2, W2–3, and W2–4, respectively.

4.6. NLFEA lateral deflection

The deflection obtained by NLFEA is indicated in Table 7. Generally, deflection showed good enhancement due to the use of ferrocement composite as compared to W1 and W2, which were reinforced with steel bars. Deflection of W1 and W2 was recorded at failure load of 2.04 mm and 4.43 mm, respectively. Enhancement varied between 21.0 % and 69.0 % for W1–1, W1–2, W1–3, and W1–4. For the second group, deflection was recorded as 2.24 mm, 5.32 mm, 1.30 mm, and 2.10 mm for W2–1, W2–2, W2–3, and W2–4, respectively. The enhancement was apparent in specimen W2–4, which had a compressive load of 1620.1 kN.

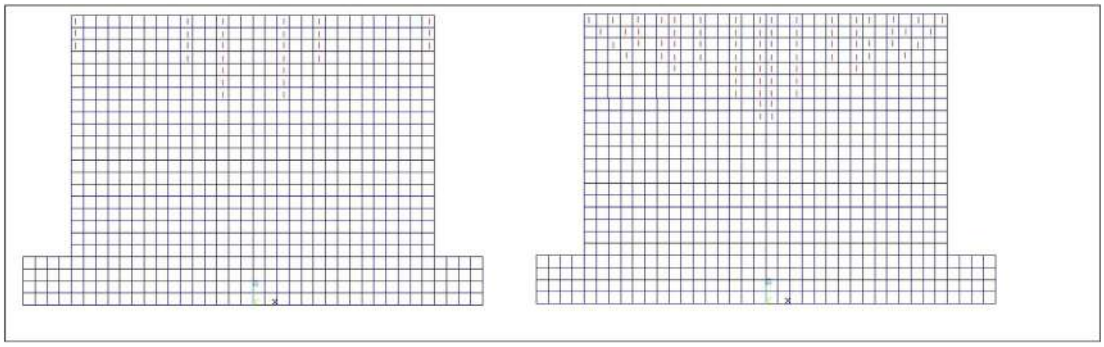

Fig. 16. Sample of NLFEA results of cracks: (a) walls under concentric loads; (b) walls under eccentric loads.

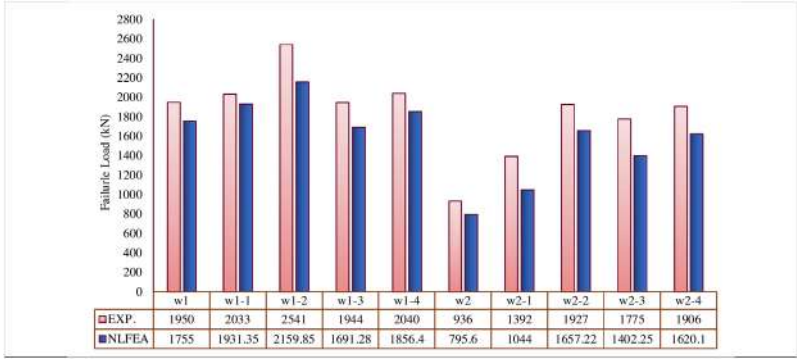

Fig. 17. Comparison between experimental and NLFEA ultimate failure load.

4.7. Crack pattern and failure mode

The crack pattern of control specimens W1 and W2 featured crack propagation in the tension zone, as shown in Fig. 16. Also, the failure mode was tension failure due to failure of reinforcement. The behavior of concrete walls reinforced with expanded ferrocement composites showed less propagation, smaller length, and lower numbers compared to walls reinforced with glass fiber ferrocement composites. This was clear upon recording the first crack in each specimen. The failure mode was tension failure, due to the ductile performance of steel and ferrocement wire mesh reinforcement.

5. Comparison between experimental and NLFEA results

Good agreement was obtained between experimental and numerical results by applying the model. Comparisons were made between failure loads, deflections, first crack loads, and crack patterns.

Table 8
Comparison between experimental and NLFEA results.

Spec. group	Symbol	Experimental load (kN)		Analytical load (kN)		Δ (mm)		$\frac{(Pu\ NLFE))}{(Pu\ (Exp))}$		$\frac{\Delta(NLFE)}{\Delta\ (Exp)}$
		First crack	Max. load	First crack	Max. load	Δ_{exp}	Δ_{NLFE}	First crack	Max. load	
Group I	W1	850.0	1950.0	320.0	1755	2.27	2.04	0.37	0.9	0.89
	W1−1	1500.0	2033.0	320.0	1931	0.65	0.62	0.21	0.95	0.95
	W1−2	1800.0	2541.0	320.0	2159	0.51	0.43	0.18	0.85	0.84
	W1−3	1020.0	1944.0	320.0	1691	1.62	1.41	0.31	0.86	0.87
Group II	W1−4	1025.0	2040.0	320.0	1856	0.61	0.55	0.31	0.91	0.90
	W2	610.0	936.0	285.0	795.6	5.21	4.43	0.47	0.85	0.85
	W2−1	620.0	1392.0	285.0	1044	2.99	2.24	0.46	0.75	0.75
	W2−2	740.0	1928.0	285.0	1657	6.19	5.32	0.38	0.86	0.86
	W2−3	648.0	1775.0	285.0	1402	1.63	1.30	0.44	0.79	0.79
Average								0.350	0.860	0.850
Variance								0.010	0.003	0.0035
Standard deviation								0.104	0.060	0.059

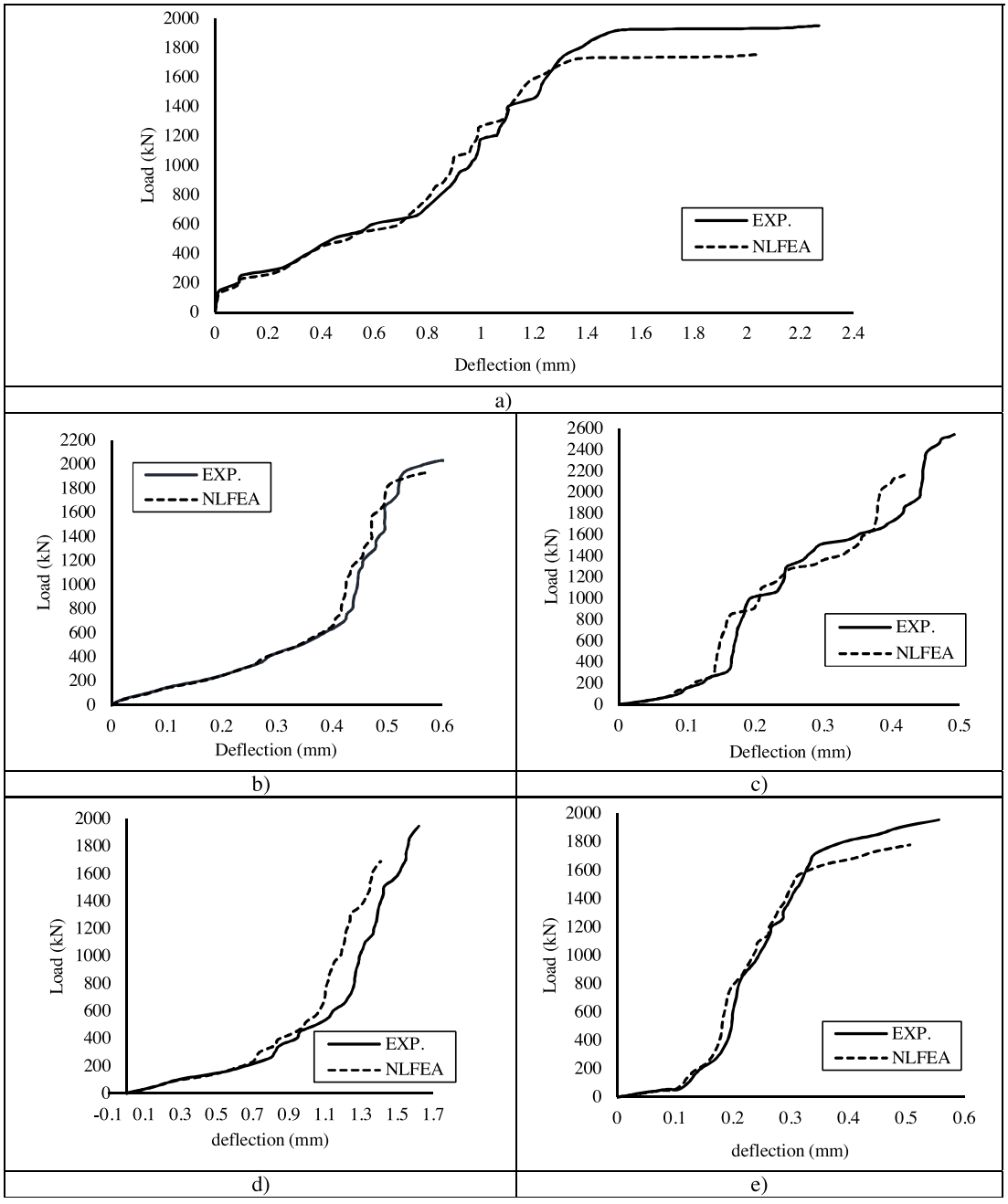

Fig. 18. Comparison of load-deflection curves under concentric load: (a) W1; (b) W1-1; (c) W1-2; (d) W1-3; (e) W1-4.

5.1. Comparison between experimental and NLFEA ultimate failure loads

Fig. 16 showed good agreement between the experimental and NLFEA load capacity, PuNLFEA / Puexp. Also, Figs. 16 & 17 showed compatibility between the experimental and analytical load–deflection curves.

Table 8 showed a comparison between the obtained experimental and NLFEA results for the different groups. The average Pu NLFEA/Pu exp. ratio is 0.86. Group II of concrete reinforced had GFRP of the same diameter but different reinforcement ratios for SP3, SP4, and SP5, and the average was 0.86. Finally, for group II the average ratio of agreement for all specimens is 0.79 and 0.91. The variance of 0.003 and standard deviation of 0.06 showed the effect of using NLFEA to predict the behavior of tested specimens, as shown in Table 8.

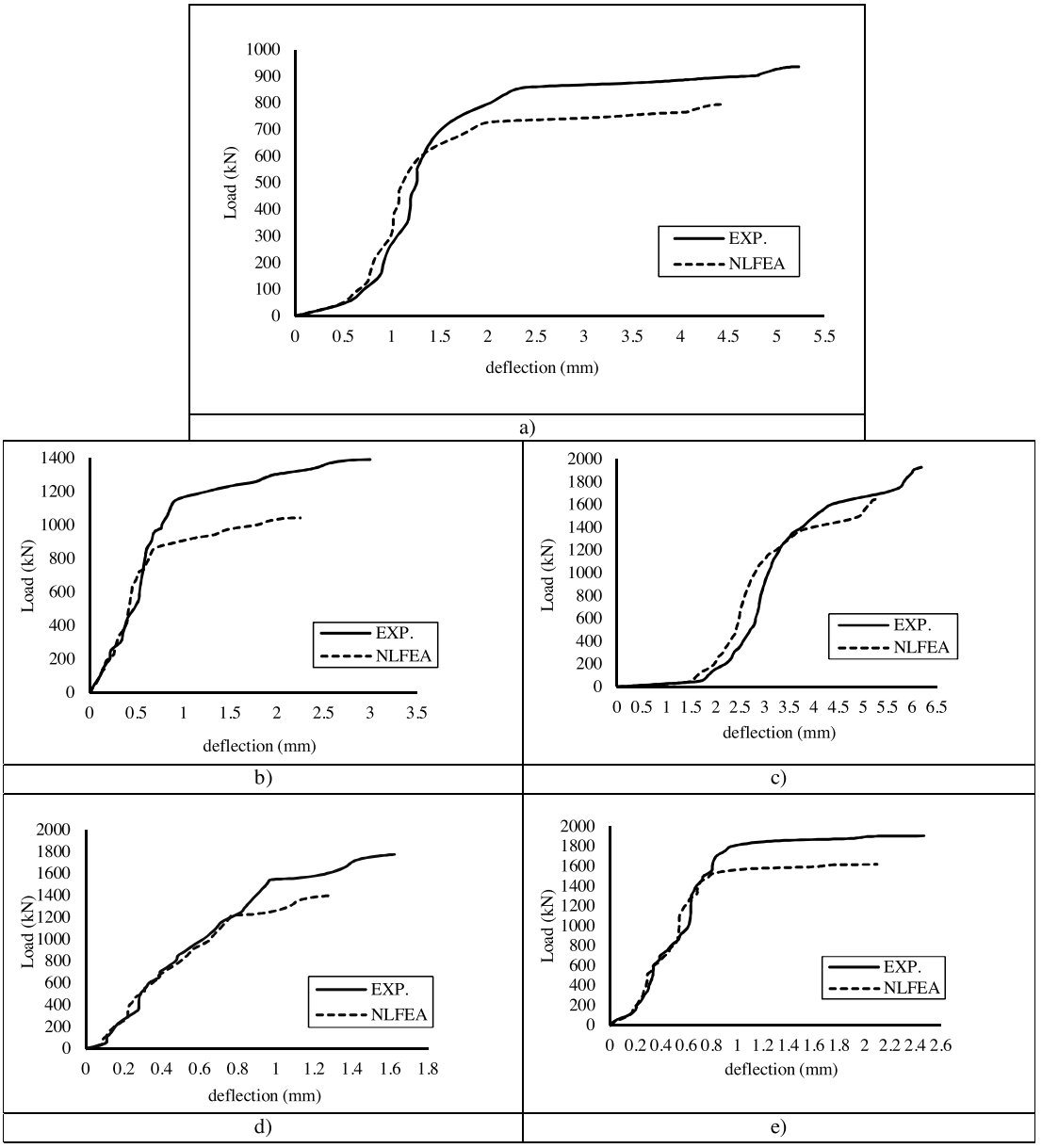

Fig. 19. Comparison of load-deflection curves under eccentric load: (a) W2; (b) W2-1; (c) W2-2; (d) W2-3; (e) W2-4.

5.2 Comparison Between Experimental and NLFEA Lateral Deflection

Figs. 17–20 showed comparison between experimental and NLFEA lateral deflection until maximum failure load. Fig. 20 showed the obtained deflection for groups in experimental and analytical studies.

The load–deflection curves for tested walls and analytical results show good agreement, with an average of 86.0 %. Table 7 shows a deflection ratio $\Delta_{u\ NLFEA}/\Delta_{u\ exp}$ of group I of 0.89, but for group II the ratio was 0.85, 0.75, 0.86, and 0.79 for W2, W2−1, W2−2, W2−3, and W2−4, respectively, and average ratio of agreement was 0.85. This indicates that the analytical model provided an acceptable load–deflection response, as shown in Table 6. For all groups, the average of $\Delta_{u\ NLFEA}/\Delta_{u\ exp}$ is equal to 0.85 with a coefficient of variance and standard deviation of 0.0035 and 0.059, respectively.

5.2. Comparison between experimental and NLFEA crack patterns and failure mode

Comparing the crack patterns of the control walls with steel reinforcement under concentric and eccentric loads, the experimental and analytical patterns feature crack propagation in the tension zone, as shown in Fig. 21, indicating tension

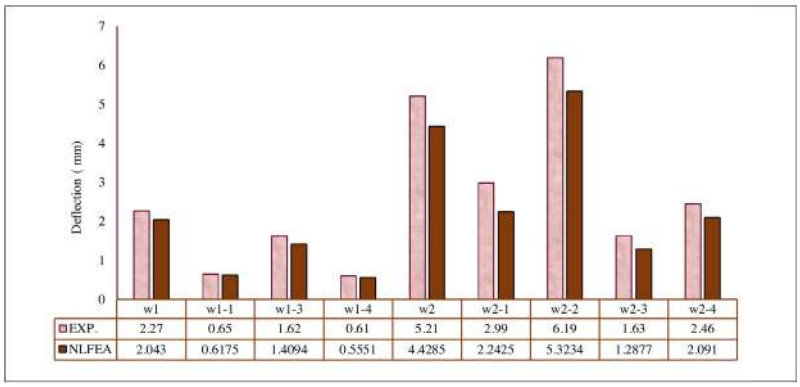

	w1	w1-1	w1-3	w1-4	w2	w2-1	w2-2	w2-3	w2-4
EXP.	2.27	0.65	1.62	0.61	5.21	2.99	6.19	1.63	2.46
NLFEA	2.043	0.6175	1.4094	0.5551	4.4285	2.2425	5.3234	1.2877	2.091

Fig. 20. Comparison between experimental and NLFEA lateral deflection.

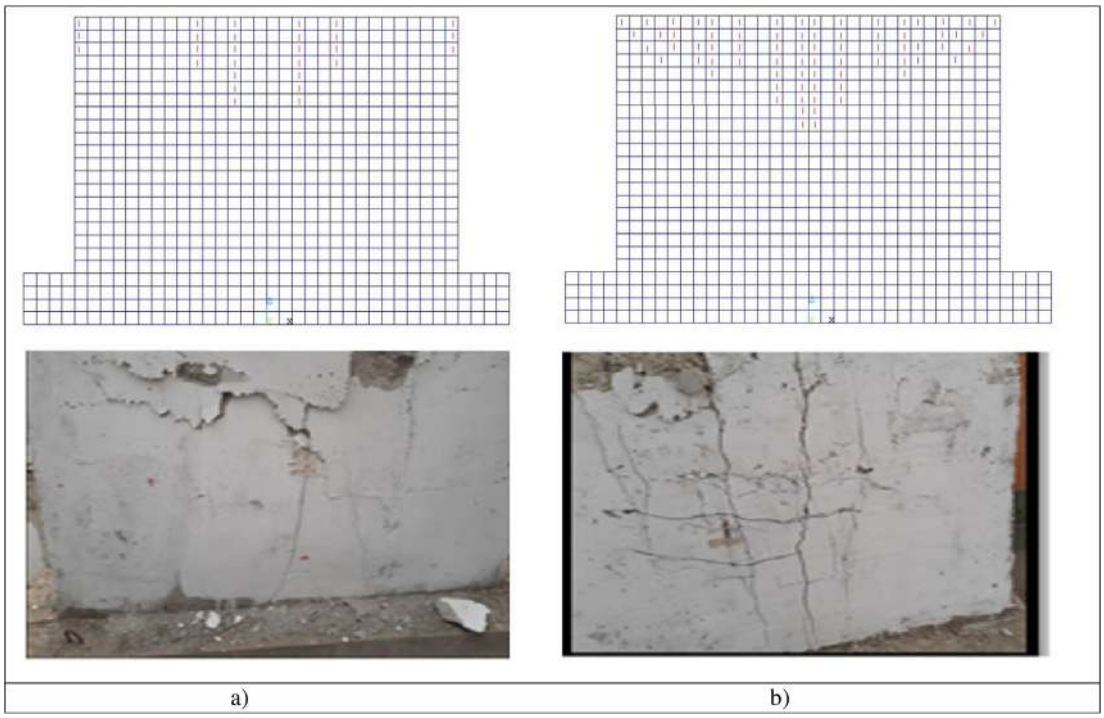

Fig. 21. Comparison between experimental and NLFEA crack patterns: (a) walls under concentric load; (b) walls under eccentric load.

failure. The crack pattern of control specimens W1 and W2 featured crack propagation in the tension zone. Also, the failure mode was tension failure due to the failure of reinforcement. The behavior of concrete walls reinforced with expanded ferrocement composites showed less propagation, shorter length, and smaller numbers compared to walls reinforced with glass fiber ferrocement composites. This was clear upon recording the first crack in each specimen. The mode of failure was tension failure, due to the ductile performance of steel and ferrocement wire mesh reinforcement. The behavior indicated high ultimate load, low deflection, and decreased cracks, showing tension cracks with low propagation as obtained from experimental patterns. The crack patterns showed good agreement between the NLFEA and experimental results.

6. Conclusions

Based on the obtained results and observations of the experimental and analytical studies presented in this paper and considering the relatively high variability and statistical pattern of data, the following conclusions can be drawn:

- Regardless the steel mesh type, expanded or glass fiber wire mesh, ferrocement specimens tested under concentric and eccentric line compression loading exhibited enhanced ultimate loads compared to control specimens.
- Changing the steel mesh type to expanded or glass fiber had the greatest effect on ultimate loads under both concentric and eccentric axial compression loading. There was a higher strength gain for specimens reinforced with expanded steel mesh, by about 111.0 %, compared with those reinforced with horizontal steel reinforcement.
- The test results show that walls with expanded wire mesh exhibited a higher ultimate load than conventionally reinforced control walls by about 105.0 % for specimens with two layers of expanded wire mesh without steel stirrups.
- The experimental results revealed that the use of increased ferrocement wire mesh as reinforcement contributed to a slightly higher ultimate load and ductility and higher energy absorption.
- Comparing the obtained lateral deflection for walls W1 and W2 with the others that had wire mesh, the deflection decreased, indicating good confinement and enhanced ductility.
- Good agreement between experimental and theoretical results was attributed to the care taken to carry out the experimental program, which could be helpful for further studies involving various parameters to be investigated.
- Glass fiber wire mesh produced a higher first cracking load, serviceability load, load carrying capacity, and energy absorption compared to expanded wire mesh.
- Using (two to four) layers of glass fiber wire mesh improved the energy absorption compared to skeletal steel bars.
- Using steel bars with one layer of expanded metal mesh improved the ductility ratio compared to two layers of expanded metal mesh only.
- Increasing the number of steel mesh layers in the ferrocement forms increased the first crack load, service load, ultimate load, and ductility ratio, decreasing the energy absorption of the walls.
- Using expanded steel wire mesh reinforcement increased the ductility ratio compared to glass fiber mesh reinforcement.

Declaration of Competing Interest

The author declare that they are no known competing financial interests or personal relationships that could have appeared to influence the work reported in this paper.

References

[1] ACI Committee 549, State-of-the-art report on ferrocement. ACI549-R97, Manual of Concrete Practice, ACI, Detroit, 2009 1997.
[2] ASTM C494/C 494 M, Standard specification for chemical admixtures for concrete, Annu. Book ASTM Stand. Sect. Water Environ. Technol. 4 (2) (2001) 9.
[3] ASTM C1116/C1116M−10a, Standard Specification for Fiber Reinforced Concrete, ASTM international, West conshohocken, PA, 2015. http://www.astm.org/.
[4] S. Bhalsing, S. Shoaib, P. Autade, Tensile strength of ferrocement with respect to specific surface, Int. J. Innov. Res. Sci. Eng. Technol. 3 (4) (2014) 501–507.
[5] J.A. Desai, Corrosion and ferrocement, Proceedings of the National Conference on Ferrocement, FS 2011, 13–14 May 2011, Pune, India, 2011, pp. 45–52.
[6] B.N. Divekar, Research needs in ferrocement technology, Proceedings of the National Conference on Ferrocement, FS 2011, 13–14 May 2011, Pune, India, 2011, pp. 227–228.
[7] Egyptian Standards Specification, E.S.S, 4756-11, Physical and Mechanical Properties Examination of Cement, Part 1, Cairo, (2012) .
[8] A.W. Hago, K.S. Al-Jabri, A.S. Alnuaimi, H. Al-Moqbali, M.A. Al-Kubaisy, Ultimate and service behavior of ferrocement roof plate panels, Constr. Build. Mater. 19 (2005) 31–37.
[9] M.A. Mansur, P. Paramasivam, Ferrocement short columns under axial and eccentric compression, Struct. Multidiscipl. Optim. 87 (5) (1990) 523–529.
[10] T. Ahmed, S.K.S. Ali, J.R. Choudhury, Experimental study of ferrocement as a retrofit material for masonry columns, Ferrocement International Symposium, (1994) , pp. 269–276.
[11] S.K. Kaushik, A. Prakash, K.K. Singh, Inelastic buckling of ferro-cement encased columns, in: Nedwell, Swamy (Eds.), Proceedings of the Fifth International Symposium on Ferrcement, London: E& FN Spon, 1994, pp. 327–341.
[12] P.J. Nedwell, M.H. Ramesht, S. Rafei-Taghanaki, Investigation into the repair of short square columns using ferro-cement, in: Nedwell, Swamy (Eds.), Proceedings of the Fifth International Symposium on Ferrcement, London: E& FN Spon, 1994, pp. 277–285.
[13] E. Fahmy, Y.B. Shaheen, Y. Korany, Repairing reinforced concrete columns using ferro-cement laminates, Journal of ferro-cement 29 (2) (1999) 115–124.
[14] E.H. Fahmy, Y.B.I. Shaheen, Y.S. Korany, Environmentally Friendly High strength concrete, Proceedings of the 24th Conference on Our World in Concrete and Structures (1999) 171–178.
[15] E.H. Fahmy, Y.B. Shaheen, M.N. Abou Zeid, H. Gaafar, Ferrocement Sandwich and cored panels for floor and wall construction, Proceedings of the 29th Conference on Our World in Concrete and Structures (2004) 245–252.
[16] E.H. Fahmy, Y.B. Shaheen, M.N. Abou Zeid, Development of ferrocement panels for floor and Wall construction, 5th Structural Specialty Conference of the Canadian Society for Civil Engineering (2004) ST218–1-ST218-10.
[17] E.H. Fahmy, M.N. Abou Zeid, Y.B. Shaheen, H. Gaafar, Behavior of ferro-cement panels under axial and flexural loadings, Proceedings of the 33rd Annual General Conference of the Canadian Society of Civil Engineering (2005) GC–150-1-GC-150-10.
[18] Alaa Abdel Tawab, Development of Permanent Formwork for Beams Using Ferro-cement Laminates P.H.D. Thesis, submitted to, Menoufia University, Egypt, 2006.
[19] R. Hazem, Non-metallic Reinforcement for the U-shaped ferro-cement forms instead of the conventional steel mesh, Deutsches Zentrum für Entwicklungstechnologien. (2009).
[20] E.H. Fahmy, B.I. Shaheen, A.M. Abdelnaby, M.N. Abou Zeid, Applying the ferro-cement concept in construction of concrete beams incorporating reinforced mortar permanent forms, Int. J. Concr. Struct. Mater. 8 (1) (2014) 83–97.
[21] S. Villar-Salinas, A. Guzmán, J. Carrillo, Performance evaluation of structures with reinforced concrete columns retrofitted with steel jacketing, J. Build. Eng. 33 (2021) 101510.
[22] P.S. Theint, A. Ruangrassamee, Q. Hussain, Strengthening of shear-critical RC columns by high-strength steel-rod collars, Eng. J. 24 (3) (2020) 107–128.
[23] Q. Hussain, A. Ruangrassamee, S. Tangtermsirikul, P. Joyklad, Behavior of concrete confined with epoxy bonded fiber ropes under axial load, Constr. Build. Mater. 263 (2020) 120093.
[24] Q. Hussain, A. Pimanmas, Shear strengthening of RC deep beams with openings using sprayed glass fiber reinforced polymer composites (SGFRP): part 1. Experimental study, Ksce J. Civ. Eng. 19 (7) (2015) 2121–2133.

[25] A. Pimanmas, Q. Hussain, A. Panyasirikhunawut, W. Rattanapitikon, Axial strength and deformability of concrete confined with natural fibre-reinforced polymers, Mag. Concr. Res. 71 (2) (2019) 55–70.
[26] K. Rodsin, Q. Hussain, S. Suparp, A. Nawaz, Compressive behavior of extremely low strength concrete confined with low-cost glass FRP composites, Case Studies in Construction Materials, (2020) , pp. e00452 13.
[27] A.A. Havez, Behaviour of PVC Encased Reinforced Concrete Walls Under Eccentric Axial Loading, University of Waterloo, Ontario, Canada, 2014.
[28] A. Chahrour, K. Soudki, RBS polymer encased concrete wall part II: experimental study and theoretical provisions for combined axial compression and flexure, Constr. Build. Mater. 20 (10) (2006) 1016–1027.
[29] ANSYS Engineering Analysis system user's Manual, Vol. 1&2, and Theoretical Manual. Revision 8.0, Swanson analysis system inc., Houston, Pennsylvania, 2005.
[30] ECP 208, Egyptian Code of Practice for Design Principles of the Use of Fiber Reinforced Polymers in Construction, Permanent Committee, 2018 Issued 2018.